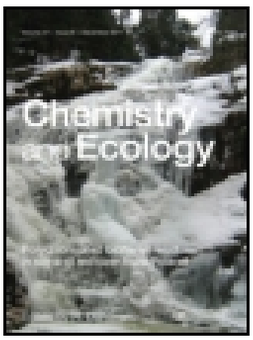

Chemistry and Ecology

ISSN: 0275-7540 (Print) 1029-0370 (Online) Journal homepage: http://www.tandfonline.com/loi/gche20

Biosorption of hexavalent chromium and malachite green from aqueous effluents, using Cladophora sp.

S. Rangabhashiyam & P. Balasubramanian

To cite this article: S. Rangabhashiyam & P. Balasubramanian (2018): Biosorption of hexavalent chromium and malachite green from aqueous effluents, using Cladophora sp., Chemistry and Ecology, DOI: 10.1080/02757540.2018.1427232

To link to this article: https://doi.org/10.1080/02757540.2018.1427232

Published online: 20 Jan 2018.

CHEMISTRY AND ECOLOGY, 2018
https://doi.org/10.1080/02757540.2018.1427232

Taylor & Francis
Taylor & Francis Group

RESEARCH ARTICLE

Biosorption of hexavalent chromium and malachite green from aqueous effluents, using *Cladophora* sp.

S. Rangabhashiyam and P. Balasubramanian

Department of Biotechnology and Medical Engineering, National Institute of Technology Rourkela, Odisha, India

ABSTRACT

Biosorption potential of green macroalgae *Cladophora* sp., (GAC) for the removal of hexavalent chromium (Cr(VI)) and malachite green (MG) from aqueous medium was investigated. Optimal conditions for biosorption experiments were determined as a function of initial pH, GAC dosage, temperature and initial concentration of Cr(VI) and MG. The biosorption equilibrium data were fitted with the isotherm models of Langmuir, Freundlich, Kiselev, Frumkin and Jovanovic, while the experimental data were analysed using the kinetic models such as pseudo-first-order, pseudo-second-order, Ritchie's and intraparticle diffusion. The Langmuir maximum biosorption capacity was calculated as 100.00 mg/g (Cr(VI)) and 142.85 mg/g (MG). The biosorption kinetic data showed better agreement with the pseudo-second-order kinetic model. The thermodynamic parameters indicated spontaneous and endothermic nature of the biosorption process for Cr(VI) removal, whereas exothermic in the case of MG removal. Furthermore, the biosorption efficiencies of the GAC reusability were found significant up to five cycles and tested using 0.1, 0.5 and 1.0 M HCl, respectively. The results of the present study indicated that GAC is a suitable biosorbent for the sequestration of Cr(VI) and MG from aqueous solutions.

ARTICLE HISTORY
Received 27 September 2017
Final Version Received 10 January 2018

KEYWORDS
Biosorption; phycoremediation; hexavalent chromium; malachite green; *Cladophora* sp.

1. Introduction

The rapid growth of industries and population increase are major responsible factors for the pollution of water bodies. The water pollution is due to the activities of untreated toxic industrial discharge and disposal of sanitary wastes. The contaminations of water are the main root cause of 70–80% diseases in the developing countries [1]. The organic and inorganic contaminants' discharge into the water bodies significantly affects the ecological balance and consequently to higher damage on the flora and fauna [2–4]. Heavy metals such as arsenic, cadmium, chromium, copper, lead, mercury, manganese, nickel and zinc in industrial effluents are inorganic contaminants discharged from the batteries, refineries, pesticides, metal plating, tanneries and mining activities. Unlike the organic pollutants, heavy metals are pronounced with more hazardous effects due to their non-biodegradable nature and higher toxicity effects [5]. Organic

CONTACT S. Rangabhashiyam rambhashiyam@gmail.com, biobala@nitrkl.ac.in Department of Biotechnology and Medical Engineering, National Institute of Technology Rourkela, Odisha 769 008, India

contaminants like dyes find applications in the industrial sectors of textile, printing, paper, leather, cosmetic and plastic. The organic dyes change aesthetic property and consumption value of the water. Moreover, dyes affect the photosynthetic activity by sunlight inhibition and cause a serious threat to aquatic organisms [6]. Nevertheless, the wider application of heavy metals and dye cannot be neglected due to their associated harmful effects under the untreated conditions. Therefore, the industrial effluent containing toxic heavy metals and dyes must be treated using a suitable method before its discharge into the environment.

Biosorption is an emerging technology used towards the removal of heavy metals and dyes from the wastewater. The merits of the biosorption process include higher efficiency, low cost and eco-friendliness [7,8]. The existing technologies of the physicochemical treatment are hurdled with the drawbacks of more requirements of chemicals' input and costlier investments [9]. Various biomaterials such as algae, fungi, bacteria and agricultural byproducts were utilised as biosorbents for the sequestrations of toxic heavy metals and dyes from the aqueous solution [10–12]. The algal biomasses are widely distributed in different habitats of marine and freshwater. Algae possess a larger large surface area and present higher affinity towards the binding of wastewater pollutants. The green algae are mainly composed of cellulose and proteins as the major constituents of the cell wall bonded to polysaccharides. The different binding groups on algal cell surface include amino, carboxyl, hydroxyl, imidazole, phosphoryl, sulphuryl, etc., which are mainly involved in the biosorption process [13]. The mechanisms of the biosorption involve ion-exchange, electrostatic attraction, covalent binding, surface precipitation, complexation, adsorption, etc. [14,15]. The benthic filamentous macroalgae *Cladophora* sp. belongs to the division of Chlorophyta. The algal biomass of *Cladophora* sp. is naturally plentiful, distributed throughout the world, one of the vital freshwater biota components plays a significant role in aquatic ecosystems and is simple to harvest [16,17].

The objectives of the present work include the evaluation of the biosorption of hexavalent chromium and malachite green (MG) using *Cladophora* sp., in the batch biosorption method. An extensive investigation into the use of *Cladophora* sp. towards the removal of hexavalent chromium and MG is not available in the literature. The influence of the biosorption parameters such as solution pH, biosorbent dosage, metal/dye concentration and temperature were studied. The biosorption isotherm and kinetic model were used to analyse the biosorption experimental data. Moreover, the thermodynamic parameters were determined.

2. Materials and methods

2.1. Biomass preparation

The biomass of green macroalgae *Cladophora* sp. was collected from the Koel river (22.32°N; 85.10°E), running in Odisha, India. The algal biomass was washed using distilled water for several times and ground to a particle size of 0.1–0.2 mm. Then the biomass was washed again with distilled water and oven dried at 60°C for 24 h. The prepared biosorbent from green algae *Cladophora* sp. (GAC) was used for the biosorption experiments without any further pretreatment.

2.2. Preparation of hexavalent chromium and MG solutions

Hexavalent chromium (Cr(VI)) and malachite green (MG) were used as target pollutants for the evaluation of removal capacity of GAC. The stock solutions of hexavalent chromium and MG were prepared by dissolving the exact quantity of potassium dichromate and powdered dyestuff in distilled water, separately. The working solutions were prepared through dilution of the stock solutions of Cr(VI) and MG to the experimental concentration ranges of 50–250 mg/L. The initial pH tuning of biosorption medium was done using 0.1 M HCl and 0.1 M NaOH.

2.3. Characterisation of GAC

The characterisation of the GAC is carried out using the instrumental analysis of Environmental Scanning Electron Microscopy (E-SEM) and Fourier Transform Infrared (FT-IR). The surface structure of the GAC was analysed using E-SEM, performed on a Quanta 250 FEG. FT-IR (Perkin Elmer Spectrum Two) spectra were used to understand the functional groups on GAC and their characteristic peak shift after interaction with hexavalent chromium and MG. The FT-IR spectra were recorded at the wavelength of 400–4000 cm^{-1}.

2.4. Experimental setup

The batch biosorption experiments were performed to determine the variation in the biosorption capacity, removal efficacy of Cr(VI) and MG from aqueous solutions with varying pH, GAC dosage, initial solute concentration and temperature. The biosorption experiments were carried out in a 250 mL Erlenmeyer flask containing GAC and 50 mL biosorbate working volume solution, and the contents were agitated at a shaking rate of 120 rpm in a thermostated shaking incubator. The samples from the biosorption medium were collected after agitation for predetermined time intervals. The equilibrium concentrations of the biosorbates were analysed using a double-beam UV–visible spectrophotometer (Systronics 2203) set at a wavelength of 540 (1,5-diphenylcarbazide) and 619 nm for Cr(VI) and MG, respectively. Kinetic biosorption studies were conducted by the GAC contact with 50 mL of initial solute concentrations of 50, 100, 150, 200 and 250 mg/L at different time intervals. The biosorption capacity of the GAC was calculated through the following expression:

$$q_t = \frac{(C_i - C_t)}{M} \times V. \tag{1}$$

The biosorption efficiency of solute removal was described in terms of percentage, using the following equation:

$$R(\%) = \left(\frac{C_i - C_t}{C_i}\right) \times 100, \tag{2}$$

where q_t is the solute biosorption capacity by GAC (mg/g), C_i is the initial solute concentration (mg/L), C_t is the solute concentration at time t (mg/L), M is the mass of biosorbent (g) and V is the solution volume (L).

2.5. Recycling experiments

The recycling of the used GAC was evaluated through the process of desorption and regeneration. The experiments of desorption were carried out using HCl with different concentrations such as 0.1, 0.5 and 1 M, respectively. The biosorbate-loaded GAC was then transferred into the 50 mL of desorption medium and the experimental conditions are followed as that of the biosorption process. The GAC after the desorption process was separated and washed many times using distilled water. The GAC is then subjected further for a biosorption study and the procedure of biosorption–desorption is repeated for five cycles.

2.6. Biosorption isotherms

The biosorption equilibrium data are suitably presented using biosorption isotherm models, which indicate a relationship between the solute concentration in the liquid phase and amount of solute biosorbed per unit mass of biosorbent at the equilibrium state. The isotherm models are characterised by specific parameters and their values represent the biosorbent surface property and affinity towards the pollutants [18,19]. To understand the isotherm model better fit on the biosorption process of Cr(VI) and MG by GAC, the acquired experimental data were analysed using the isotherm models. In the present study, five different biosorption isotherm models such as Langmuir, Freundlich, Kiselev, Frumkin and Jovanovic were subjected to correlate the biosorption experimental data.

2.6.1. Langmuir biosorption isotherm

The Langmuir isotherm model indicates the homogenous biosorption surface with uniform energies in the biosorbent active sites. This model based on the assumption of biosorbent surface as homogenous containing equivalent site presents monolayer biosorption with negligible interactions between the solutes [20]. The linear form of the Langmuir isotherm model is represented by

$$\frac{1}{q_e} = \left(\frac{1}{K_L Q_0}\right)\frac{1}{C_e} + \frac{1}{Q_0}, \tag{3}$$

where Q_0 (mg/g) is the maximum value of solute biosorption per unit biosorbent weight, which denotes the monolayer biosorption capacity, and K_L (L/mg) indicates the Langmuir isotherm constant, which refers to the solute affinity to the biosorbent.

The Langmuir isotherm shape can be predicted using separation factor (R_L), which is a dimensionless constant useful to analyse the favourability of Langmuir isotherm for the biosorption equilibrium data [21]. The separation factor (R_L) calculated using the following equation:

$$R_L = \frac{1}{1 + K_L C_i}. \tag{4}$$

The value of R_L between 0 and 1 represents the favourable biosorption; R_L value greater than 1 specifies unfavourable biosorption. R_L equal to 1 denotes linear biosorption, and irreversible biosorption occurs in case of R_L value equal to zero.

2.6.2. Freundlich biosorption isotherm

The Freundlich isotherm is the most primitive known empirical equation describing the biosorption equilibrium. The isotherm reports biosorption on the heterogeneous surface and the assumption includes a logarithmic decrease in the biosorption enthalpy with an increase in the fraction of occupied sites on the biosorbent [22]. The linear expression of the Freundlich isotherm model is given as follows:

$$\log q_e = \log K_F + \frac{1}{n}\log C_e, \tag{5}$$

K_F (mg/g) represents the Freundlich isotherm constant related to biosorption capacity. The Freundlich isotherm constant, n, indicates the surface heterogeneity. The higher value of n denotes the biosorption system as more heterogeneous.

2.6.3. Kiselev biosorption isotherm

The Kiselev biosorption isotherm is based on the assumption that the biosorption process occurs in localised monomolecular layer [23], the linear form of this isotherm is given below:

$$\frac{1}{C_e(1-\theta)} = \frac{K_{KL}}{\theta} + K_{KL}K_n, \tag{6}$$

θ represents the surface coverage [$\theta = (1 - C_e/C_i)$], K_{KL} (L/mg) is the Kiselev isotherm model equilibrium constant and K_n is the constant of complex formation between biosorbed molecules.

2.6.4. Frumkin biosorption isotherm

The Frumkin isotherm model elucidates the interaction between adjacent biosorbed molecules within the monolayer [24]. The linear form of the Frumkin isotherm model is expressed as follows:

$$\ln\left[\left(\frac{\theta}{1-\theta}\right)\frac{1}{C_e}\right] = \ln K + 2a_F\theta, \tag{7}$$

K is the equilibrium constant of Frumkin isotherm model and a_F is the Frumkin interaction parameter between the biosorbed molecules. The value of a_F can be either positive or negative. The positive value of a_F denotes the increased biosorption energy because of lateral attraction between the biosorbed molecules, and the negative value of a_F suggests the presence of lateral repulsive force between the molecules in the biosorbed layer.

2.6.5. Jovanovic biosorption isotherm

The Jovanovic isotherm model is primarily subjected for the studies on gas adsorption. This isotherm model assumption is the same as that of the Langmuir isotherm except the additional consideration over the possibility on the existence of mechanical contacts between the biosorbing and desorbing molecules in the case of homogenous surface [25]. The Jovanovic isotherm model is represented by

$$\ln q_e = \ln q_{mj} - K_j C_e, \tag{8}$$

where K_j (L/g) represents Jovanovic constant, related to biosorption energy and q_{mj} (mg/g) is the maximum biosorption capacity.

2.7. Biosorption kinetics

The kinetic models were used to investigate the mechanisms and rate-controlling step of the pollutant removal process by biosorption. The kinetic models of pseudo-first-order, pseudo-second-order, Ritchie's and intraparticle diffusion were tested with experimental data of the biosorption study.

2.7.1. Pseudo-first-order model

The pseudo-first-order kinetic model is also referred to as the Lagergren [26] first-order rate expression, based on the biosorption capacity. The integral form of pseudo-first-order rate is given by

$$\log (q_e - q_t) = \log q_e - \frac{k_1}{2.303} t, \tag{9}$$

where q_e (mg/g) is the biosorption amount at equilibrium, q_t (mg/g) is the biosorption amount at time t in min and k_1 (min^{-1}) denotes the pseudo-first-order rate constant.

2.7.2. Pseudo-second-order model

The kinetic model of pseudo-second-order, based on the assumption of chemisorption, is the dominant mechanism, which controls the biosorption as a rate-limiting step. The linear form of pseudo-second-order kinetic model [27] applied is

$$\frac{t}{q_t} = \frac{1}{k_2 q_e^2} + \frac{t}{q_e}, \tag{10}$$

where k_2 (g/mg min) is the pseudo-second-order rate constant.

2.7.3. Ritchie's model

The Ritchie kinetic model [28] assumes that the biosorption rate mainly depends on the fraction of unoccupied sites on the biosorbent. The linear form of the equation is expressed as follows:

$$\frac{1}{q_t} = \frac{1}{k_R q_e t} + \frac{1}{q_e}, \tag{11}$$

where k_R (min^{-1}) is the rate constant of the Ritchie kinetic model.

2.7.4. Intraparticle diffusion

The Weber–Morris equation derived from Fick's law establishes a relationship between biosorbent uptake and square root of biosorption time [29]. The equation of intraparticle diffusion kinetic model is written as follows:

$$q_t = k_{id} t^{1/2} + C, \tag{12}$$

where k_{id} (mg/g min$^{1/2}$) indicates the rate constant of intraparticle diffusion model and C (mg/g) is the intercept.

2.8. Biosorption thermodynamics

The influences of temperature in the biosorption process analysed using the van't Hoff equation, which is used to determine the thermodynamic parameters. The integrated form of the van't Hoff equation is represented by

$$\ln K_C = \frac{-\Delta H^\circ}{RT} + \frac{\Delta S^\circ}{R}, \% \tag{13}$$

where K_C is the equilibrium constant, ΔH° (kJ/mol) is the standard enthalpy change, ΔS° (kJ/mol/K) is the standard entropy change, T (K) is the absolute temperature and R (8.314 J/mol K) is the universal gas constant. ΔG° (kJ/mol) indicates the standard Gibbs free energy change calculated according to the following equation:

$$\Delta G^\circ = -RT \ln K_C. \tag{14}$$

3. Results and discussion

3.1. Effect of pH on Cr(VI) and MG biosorption

The initial pH of the aqueous solution is one of the important parameters in the biosorption process. The pH of the biosorption system influences on the biosorbent surface properties and causes the ionisation or dissociation of the biosorbate molecule. Figure 1 represents the variations in the removal of Cr(VI) and MG from aqueous solution at the initial solution pH range from 2.0 to 10.0. It can be observed that the biosorption of Cr (VI) is highly dependent on the solution pH. At the initial solution pH 2.0, GAC showed highest removal efficiency of 96.85% and biosorption capacity of 34.59 mg/g, towards the removal of Cr(VI). For the increase of pH from 2.0 to 5.0, the biosorption efficiency and capacity significantly reduced to 14.55% and 40.74 mg/g. The further pH increase from 5.0 to 10.0 did not show obvious changes in Cr(VI) removal performance by GAC. At the lower pH of the biosorption medium, the negatively charged chromium ions interacts with positively charged GAC surface by means of electrostatic attraction. The increase

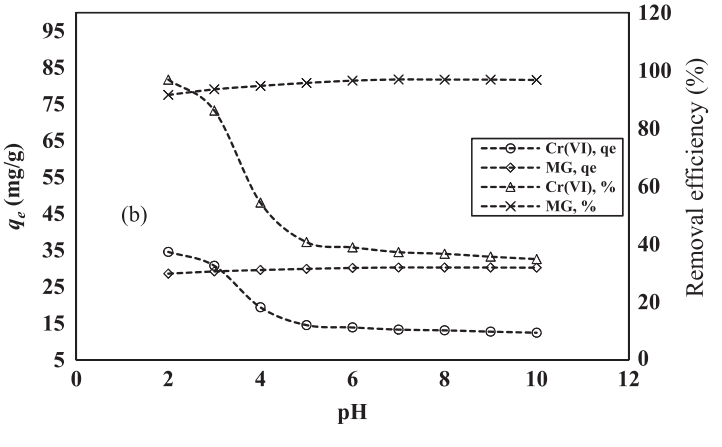

Figure 1. Plots showing the effect of initial pH on the biosorption capacity and percentage removal of Cr(VI) and MG using GAC.

of pH caused the GAC surface negative and consequent to decline in the biosorption of Cr (VI) [30]. The influence of solution pH on the removal of MG using GAC was shown in Figure 1. The MG removal was higher at pH 7.0 with 96.94% biosorption efficiency and biosorption capacity of 30.29 mg/g. The results at the solution pH 2.0 showed a slightly decreased removal efficiency and biosorption capacity because the positively charged GAC surface leads to electrostatic repulsion and more number of H^+ ions compete with MG for the biosorption sites on the biosorbent [31]. Therefore, initial pH of 2.0 and 7.0 was selected for the Cr(VI) and MG biosorption experiments.

3.2. Effect of GAC dosage on Cr(VI) and MG biosorption

The biosorbent dosage determination is important in the potential evaluation of biosorbent towards solute removal at a fixed concentration. The influence of amount of GAC for the biosorption of Cr(VI) and MG is shown in Figure 2. The study was conducted by changing the biosorbent dosage from 0.01 to 0.1 g with the fixed initial solute concentration of 50 mg/L. Figure 2 indicated that the percentage removal of Cr(VI) and MG increased from 41.07% to 96.85% and 86.04% to 96.94%, respectively, for the increase of GAC dosage from 0.01 to 0.1 g. The results are attributed to the availability of more biosorptive surface area and higher number of the interactive sites offered by the GAC [32]. The biosorbent dosage increases beyond 0.07 and 0.08 g for GAC–Cr(VI); GAC–MG did not show notable changes in the removal process. Moreover, the biosorption capacity of GAC towards the removal of Cr(VI) and MG showed a decreased effect with an increase in the biosorbent dosage under the condition of constant C_i. This may be because of an increase in diffusion path length, unsaturation, overlapping or aggregation of biosorption sites [33].

3.3. Effect of temperature and thermodynamics parameters

In order to evaluate the temperature effect on the biosorption performance of GAC for the removal of Cr(VI) and MG, the experiments were performed at 303, 313, 323 and 333 K for the initial solute concentration range of 50–250 mg/L. Figure 3 presents the biosorption

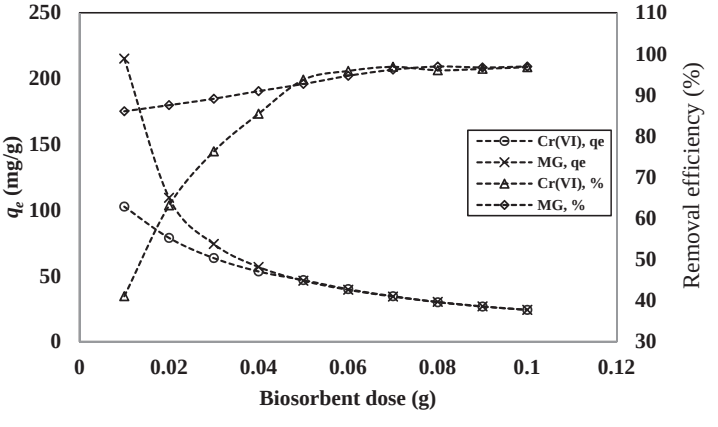

Figure 2. Plots showing the effect of GAC dosage on the uptake capacity and percentage removal of Cr (VI) and MG from aqueous solution.

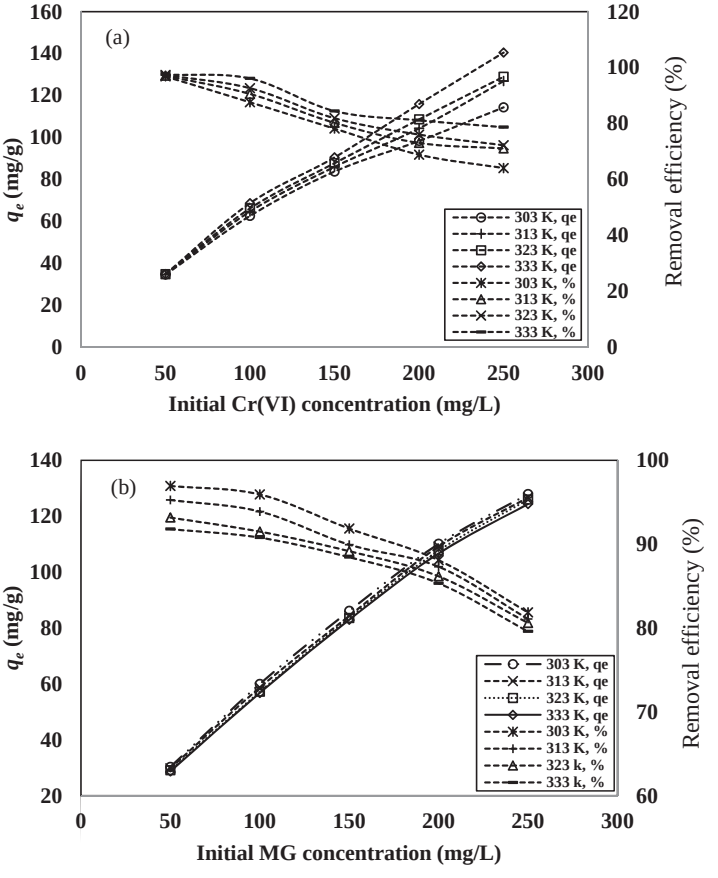

Figure 3. Plots showing the temperature effect on the biosorption of (a) Cr(VI) and (b) MG at different initial concentrations using GAC.

profiles of Cr(VI) and MG using GAC at different temperatures. With the increase in temperature, the biosorption capacity and the percentage removal of Cr(VI) was found enhanced for all the concentrations considered. These effects may be due to an increase in the biosorbent active sites and a reduction in the boundary layer thickness of the biosorbent, which offers reduced mass transfer resistance for Cr(VI) ions [34]. In the case of the MG biosorption by GAC, the temperature increase from 303 to 333 K showed a negative effect for the initial concentration range of 50–250 mg/L. Higher biosorption capacity and percentage removal was observed at 303 K for biosorption of MG using GAC. The decreased biosorption effects with increase in temperature are due to the bond weakening between MG and GAC binding sites.

Using Equation (14), the values of ΔG° for the biosorption of Cr(VI) and MG were calculated for different temperatures. The values of ΔH° and ΔS° were found using the van't Hoff plot of ln K_c versus 1/T (Figure 4). The calculated values of thermodynamic parameters are given in Table 1. The thermodynamic analysis of Cr(VI) biosorption showed a decrease in the values of ΔG° with the increase of temperature for all the initial Cr(VI) concentration, which indicates that the biosorption process was feasible and spontaneous. Further, the positive values of ΔH° suggested the biosorption process as endothermic in nature, and

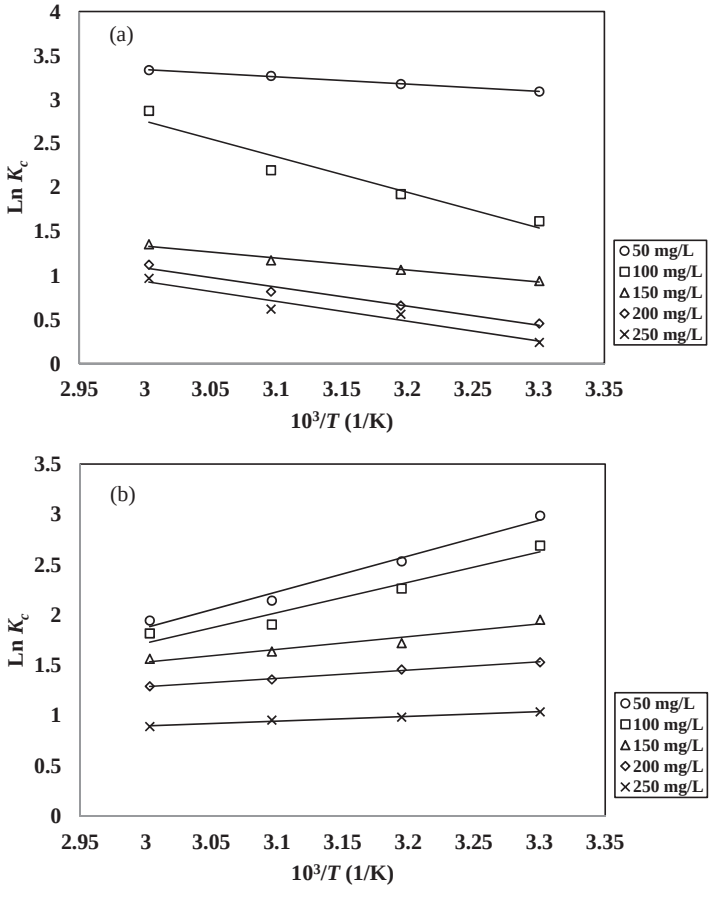

Figure 4. The plot of ln K_c versus 1/T for (a) Cr(VI) and (b) MG biosorption onto GAC.

the positive values of ΔS° represented higher affinity of GAC and the increasing randomness at the interface of solid solution during the biosorption of Cr(VI) onto GAC [35]. In the case of MG biosorption using GAC, an increase in ΔG° values observed with increase in temperature represented the biosorption process as not feasible and thermodynamically non-spontaneous. Moreover, the negative values of ΔH° parameter indicated exothermic nature of the biosorption process. The ΔS° parameter values were found negative for all the temperatures and initial MG concentrations considered in the present study suggested the effect of decreased randomness at the solid/solution interface during the MG bisorption.

3.4. Effect of initial solute concentration and biosorption isotherms

The effect of initial solute concentration on biosorption of Cr(VI) and MG studied within the range of 50–250 mg/L and the results are presented in Figure 5. The plots showed that the amount of solute retained on GAC increased with initial solute concentration increase from 50 to 250 mg/L, whereas the biosorption removal efficiencies showed decreased effect in the case of both Cr(VI) and MG removal. The increasing trend of uptake capacity may be

Table 1. Thermodynamic parameters for biosorption of Cr(VI) and MG onto GAC.

		Cr(VI) biosorption					MG biosorption		
Temperature (K)	C_i (mg/L), Cr (VI)	$\Delta G°$ (kJ/mol)	$\Delta H°$ (kJ/mol)	$\Delta S°$ (kJ/mol K)	Temperature (K)	C_i (mg/L), MG	$\Delta G°$ (kJ/mol)	$\Delta H°$ (kJ/mol)	$\Delta S°$ (kJ/mol K)
303	50	−7.790	6.898	0.048	303	50	−7.526	−29.614	−0.073
313		−8.267			313		−6.590		
323		−8.779			323		−5.756		
333		−9.234			333		−5.384		
303	100	−4.078	33.588	0.123	303	100	−6.775	−25.108	−0.061
313		−5.013			313		−5.887		
323		−5.899			323		−5.118		
333		−7.951			333		−5.030		
303	150	−2.367	11.348	0.045	303	150	−4.919	−10.533	−0.018
313		−2.772			313		−4.477		
323		−3.150			323		−4.397		
333		−3.755			333		−4.333		
303	200	−1.149	18.049	0.063	303	200	−3.855	−6.859	−0.009
313		−1.720			313		−3.794		
323		−2.196			323		−3.650		
333		−3.111			333		−3.573		
303	250	−0.6072	18.773	0.064	303	250	−2.611	−3.933	−0.004
313		−1.463			313		−2.563		
323		−1.663			323		−2.562		
333		−2.683			333		−2.464		

due to the role of initial concentration acts as a driving force in such a way to overcome mass transfer resistance for the transport of solute molecules between the aqueous solution and GAC surface. The lower biosorption efficiency at higher concentrations of Cr (VI) and MG might be because of the decline of interaction sites on the GAC for the biosorption [36].

The parameters of biosorption isotherms models and the coefficient of determination (R^2) values are given in Table 2. Based on the analysis of R^2 values obtained for the biosorption equilibrium data fit with two parameter isotherm models, the Langmuir isotherm model better described the removal process of MG ($R^2 = 0.996$) and the Freundlich isotherm model showed best fit of the Cr(VI) equilibrium data ($R^2 = 0.998$). The values of

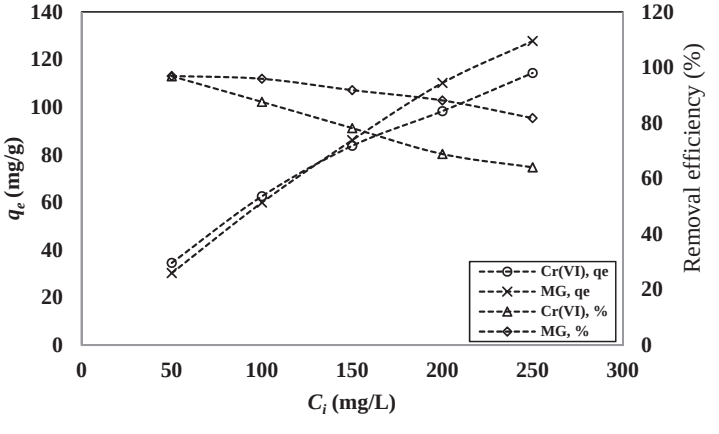

Figure 5. Plots showing the effect of initial solute concentration on the biosorption capacity and percentage removal of Cr(VI) and MG using GAC.

Table 2. Isotherm model parameters for the removal of Cr(VI) and MG using GAC.

Isotherm model	Parameters	Cr(VI) biosorption	MG biosorption
Langmuir	Q_0	100.00	142.85
	K_L	0.3448	0.1842
	R^2	0.943	0.996
Freundlich	K_F	30.1995	28.9067
	n	3.4364	2.4154
	R^2	0.998	0.961
Kiselev	K_{KL}	−28.52	−79.39
	K_n	−1.4414	−1.1768
	R^2	0.475	0.460
Frumkin	K	3.52×10^{-8}	6.93×10^{-14}
	a_F	9.955	16.795
	R^2	0.932	0.920
Jovanovic	K_J	−0.011	−0.026
	q_{mj}	45.92	46.47
	R^2	0.791	0.685

the separation factor were found as 0.0548–0.0114 (Cr(VI)) and 0.0979–0.0212 (MG) for the initial solute concentration range of 50–250 mg/L. The values of R_L obtained for the studied initial solute concentrations were between 0 and 1 (Figure 6), which confirms the biosorption of Cr(VI) and MG onto GAC as a favourable process. The maximum biosorption capacity according to the Langmuir isotherm model was determined as 100.00 and 142.85 mg/g for the removal of Cr(VI) and MG using GAC. For comparison (Table 3), the biosorption capacity of GAC towards Cr(VI) and MG removal was found higher than those of other biosorbents reported in the literature.

It can be observed from Table 2 that the values of the Freundlich isotherm constant, n, were greater than unity, which shows that the Cr(VI) and MG were favourably biosorbed by GAC. Based on the R^2 value results of all the two parameters isotherms considered in this study, the following order of best-fitted isotherm was observed for Cr(VI) biosorption by GAC, Freundlich > Langmuir > Frumkin > Jovanovic > Kiselev. In the case of MG biosorption using GAC, the order of the best-fitted isotherm is as follows: Langmuir > Freundlich > Frumkin > Jovanovic > Kiselev. For both Cr(VI) and MG biosorption equilibrium data, Kiselev isotherm is the least fitted model.

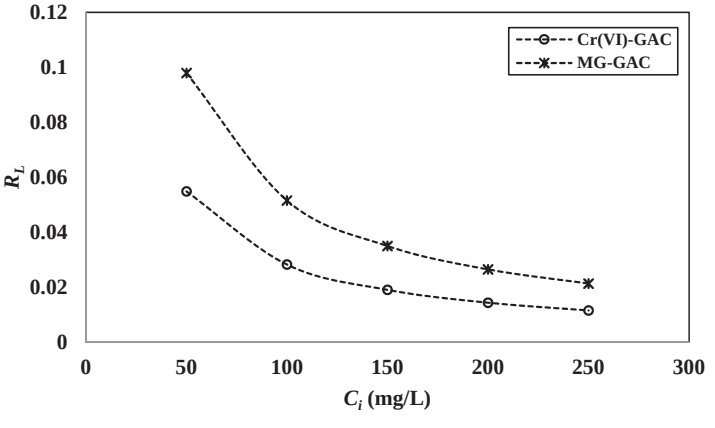

Figure 6. Langmuir separation factor profile for biosorption of Cr(VI) and MG as a function of initial solute concentration using GAC.

Table 3. Comparison of biosorption capacities of different biosorbents with GAC for Cr(VI) and MG removal.

	Biosorbent	Biosorption capacities (mg/g)	References
Cr(VI) biosorption	*Spirogyra condensata*	14.82	[37]
	Oedogonium hatei	31.00	[38]
	Sterculia guttata shell	45.45	[39]
	Melaleuca diosmifolia leaf	62.5	[40]
	Peganum Harmala	10.63	[41]
	GAC	100.00	Present study
MG biosorption	*Pithophora* sp.	117.647	[42]
	Walnut shell	90.8	[43]
	Potato peel	32.39	[44]
	Pomegranate peel	31.45	[45]
	Carica papaya wood	52.63	[46]
	GAC	142.85	Present study

3.5. Biosorption kinetics

The pseudo-first-order, pseudo-second-order, Ritchie's and Intraparticle diffusion kinetic models were subjected to analyse the biosorption experimental data of Cr(VI) and MG removal. Table 4 presents the results of experimentally determined equilibrium biosorption capacity ($q_{e\ (exp)}$) and kinetic model parameters along with R^2 values. Upon comparing R^2 values obtained for all the kinetic models used in the present study, the pseudo-second-order kinetic model was found to exhibit the highest R^2 values for biosorption data of both Cr(VI) and MG removal using GAC. Further, the pseudo-second-order kinetic model predicted equilibrium biosorption capacity matched closely with the values of experimentally determined equilibrium biosorption capacity. Similarly, Ritchie's model $q_{e\ (cal)}$ values are found closely matched with the values of $q_{e\ (exp)}$, but R^2 values were observed comparatively lesser than the pseudo-second-order kinetic model.

For the increase in initial concentration of Cr(VI) and MG from 50 to 250 mg/L, the values of pseudo-second-order kinetic rate constant (k_2) are found slightly decreased (Table 4). The decrease in k_2 value at the higher concentrations of Cr(VI) and MG may be due to slower rate biosorption equilibrium uptake at the higher solute concentrations because of the availability of limited binding sites on the GAC surface. Therefore, the pseudo-second-order kinetic model was selected as the most appropriate kinetic model for describing the biosorption kinetics of Cr(VI) and MG using GAC. The pseudo-second-order kinetic model based on the assumption that two surface sites on the biosorbent will undergo interaction with one biosorbate ion. The pseudo-second-order kinetic model best fits with the biosorption data and revealed that the chemisorption mechanism [47] is most likely to be the rate-determining step of the overall rate of Cr(VI) and the MG biosorption process.

3.6. E-SEM and FT-IR analysis

The micrographs of E-SEM analysis performed are shown in Figure 7. The E-SEM images demonstrate the presence of superficial porous structure with rugged morphology; moreover, the filaments of the algal biomass are bonded together. The uneven structure of GAC offers good accessibility for Cr(VI) and MG, into the interior and surface structure of GAC biosorbent. In order to examine the interactions between the GAC surface functional

Table 4. Kinetic model parameters for removal of Cr(VI) and MG by GAC.

		Initial concentration									
		Cr(VI)	MG	Cr(VI)	MG	Cr(VI)	MG	Cr(VI)	MG	Cr(VI)	MG
Model	Parameters	50 (mg/L)		100 (mg/L)		150 (mg/L)		200 (mg/L)		250 (mg/L)	
	$q_{e(exp)}$	34.59	30.29	62.57	59.95	83.76	86.11	98.34	110.10	114.37	127.90
Pseudo-first-order	k_1	0.0829	0.0621	0.0506	0.0552	0.0552	0.0552	0.0667	0.0368	0.0598	0.0621
	$q_{e(cal)}$	29.10	9.22	38.99	19.36	42.65	24.88	50.46	39.53	68.86	111.68
	R^2	0.958	0.807	0.891	0.791	0.842	0.755	0.892	0.669	0.895	0.839
Pseudo-second-order	k_2	0.0072	0.0262	0.0030	0.0098	0.0031	0.0080	0.0045	0.0022	0.0022	0.0028
	$q_{e(cal)}$	37.03	31.25	66.66	62.50	90.90	90.90	100.00	125.00	125.00	142.00
	R^2	0.999	1.000	0.998	0.999	0.999	0.999	0.999	0.999	0.999	0.999
Ritchie's	k_R	0.2596	1.2222	0.2777	1.0000	0.4230	1.1000	0.5263	0.5625	0.0230	0.5833
	$q_{e(cal)}$	37.03	30.30	66.66	62.50	90.90	90.90	100.00	111.111	125.00	142.85
	R^2	0.905	0.883	0.849	0.871	0.819	0.905	0.925	0.847	0.881	0.849
Intraparticle diffusion	k_{id}	1.022	0.269	1.952	0.653	1.872	0.838	1.757	2.077	2.889	2.116
	C	25.18	27.68	43.96	53.58	66.06	77.97	81.83	89.16	86.90	107.6
	R^2	0.752	0.896	0.863	0.928	0.890	0.879	0.829	0.930	0.848	0.889

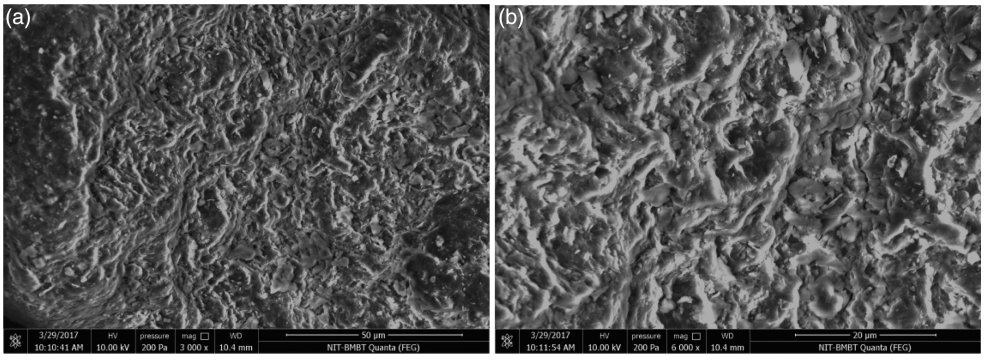

Figure 7. E-SEM images of GAC under (a) 3000× and (b) 6000× magnifications.

groups and Cr(VI) and MG, the samples of the GAC- and solute-loaded GAC were analysed using FT-IR spectroscopy (Figure 8). Figure 8 displays intense characteristic bands in GAC, which indicates the presence of different functional groups from the biomolecules of

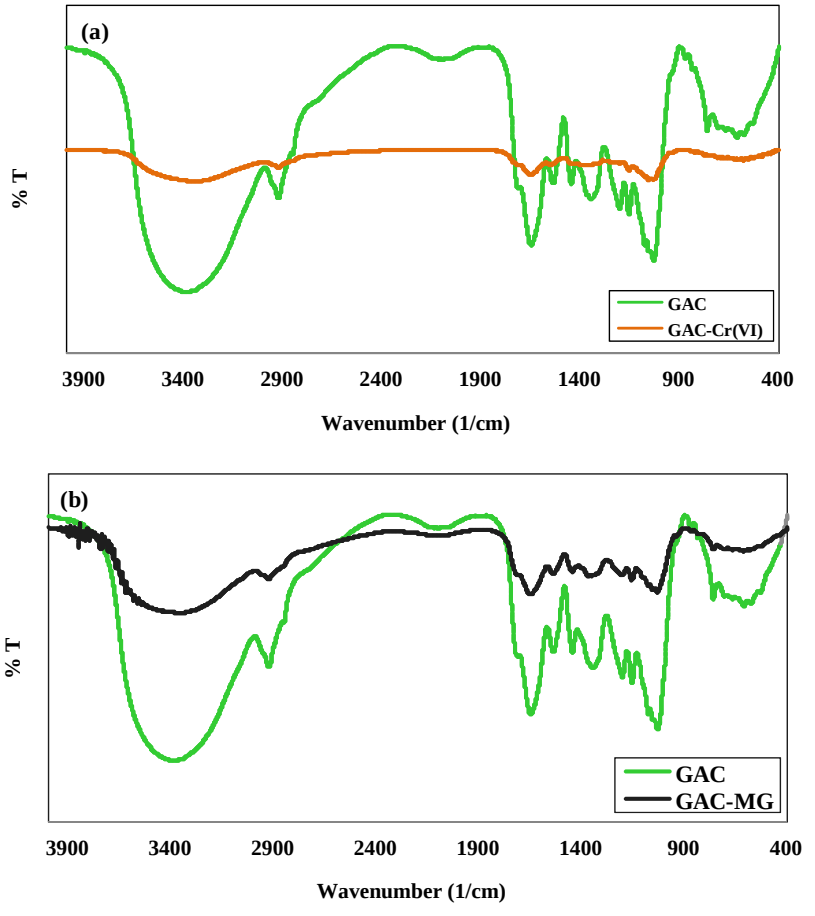

Figure 8. FT-IR spectra of GAC loaded with (a) Cr(VI) and (b) MG.

polysaccharides and proteins. The broad band around 3800–3000 cm^{-1} represents the presence of the hydroxyl (–OH) groups and amine (–NH) groups on GAC [48]. The peak at 2927 cm^{-1} is attributed to the symmetric and asymmetric C–H stretching vibrations of the aliphatic groups from lipids. The strong peaks observed at 1650 cm^{-1} corresponds to the stretching vibration of the carboxyl group (–C=O). The peak at 1447 cm^{-1} indicates the bending vibrations of –N–H group. The band at 1351 cm^{-1} is assigned to Nitroso (–N=O) stretching vibrations. The band observed at 1033 cm^{-1} is identified as the functional group of C–O–C, which reveals polysaccharides distribution in the GAC biomass [49].

The FT-IR spectra comparison of Cr(VI) (Figure 8(a)) and MG-loaded GAC (Figure 8(b)) with reference to the unloaded GAC displayed significant shifts in some of the peak

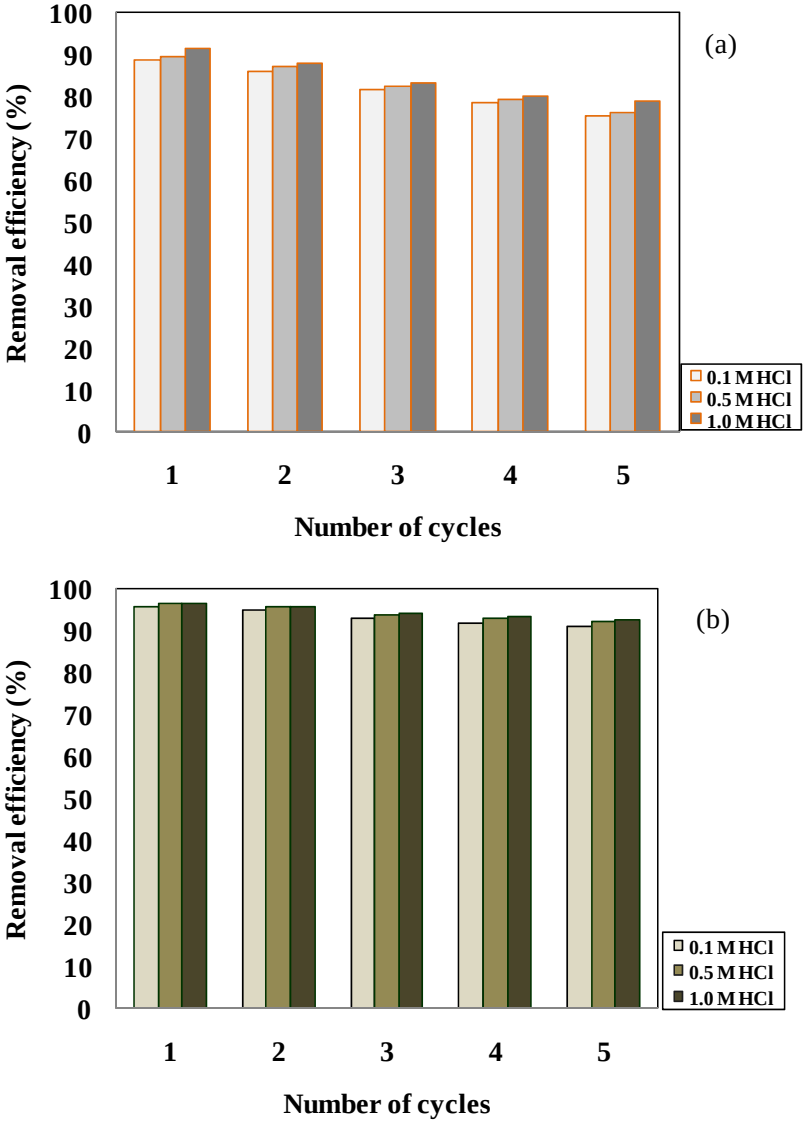

Figure 9. Reusability of GAC for (a) Cr(VI) and (b) MG biosorption.

regions. The peaks at 3384 and 1351 cm^{-1} (GAC) were shifted to 3347, 1370 cm^{-1} (Cr(VI)-loaded GAC) and 3568, 1371 cm^{-1} (MG-loaded GAC), respectively, which suggested that hydroxyl, amine and nitroso functional groups are mainly contributed in the biosorption of Cr(VI) and MG using GAC.

3.7. Desorption and reuse efficiency

The desorption of Cr(VI) and MG from the GAC was investigated to determine the reusability of GAC for the biosorption recycles. The results of reusability performance of GAC for the removal of Cr(VI) and MG from an aqueous solution up to five cycles are depicted in Figure 9. After each biosorption study, GAC was recovered with the desorbing agent HCl (0.1, 0.5 and 1.0 M), washed with distilled water and subjected for recycling. The results revealed that 1.0 M HCl desorbing agent showed better removal efficiency up to five cycles with no significant loss of activity in MG removal compared to the Cr(VI) biosorption. Therefore, the performance of GAC validates its recyclability in the biosorptive process of Cr(VI) and MG.

4. Conclusion

The present study carried out an investigation on the biosorptive removal of Cr(VI) and MG using green macroalgae *Cladophora* sp. The parametric effects on the biosorption process were analysed and optimal conditions were determined. Initial pHs of 2.0 and 7.0 were found as the optimum values for the better removal of Cr(VI) and MG by GAC. At the biosorption temperature of 333 K, higher removal of Cr(VI) was observed and for the MG biosorption, there observed a decline in the biosorption efficiency with the increase of temperature from 303 to 333 K. The estimated values of the thermodynamic parameters showed that the biosorption of Cr(VI) onto GAC was feasible, spontaneous and endothermic. In contrast, the thermodynamic parameters of MG removal indicated non-spontaneous and exothermic nature of biosorption process. The biosorption equilibrium data of Cr(VI) and MG were better fitted with the Langmuir and Freundlich isotherm model. The maximum biosorption capacity was found as 100.00 and 142.85 mg/g for Cr (VI) and MG, respectively. The kinetics of the biosorption process of both Cr(VI) and MG obeyed the pseudo-second-order kinetic model. The reusability of the GAC demonstrates its potential in recycle for biosorption process up to five cycles without loss of biosorption efficiency. The present investigation demonstrated that GAC is an alternative eco-friendly biosorbent for the removal of hexavalent chromium and MG from an aqueous solution.

Acknowledgements

The authors are thankful to the Department of Biotechnology and Medical Engineering, National Institute of Technology Rourkela for the research facility.

Disclosure statement

No potential conflict of interest was reported by the authors.

Funding

This project is funded by the Science and Engineering Research Board, Department of Science and Technology, India [grant number PDF/2016/000284].

Notes on contributors

Dr S. Rangabhashiyam presently working as postdoctoral researcher in the Department of Biotechnology and Medical Engineering, National Institute of Technology Rourkela, India. He has published more than 30 articles. As a first author, he published 17 articles including both review and research in the relevance of biosorption. He has explored many plant and algal biomasses in the natural and modified form, and subjected them towards the removal of toxic heavy metals, dyes from aqueous solutions and industrial effluents.

Dr P. Balasubramanian is serving as Assistant Professor in Department of Biotechnology and Medical Engineering of National Institute of Technology Rourkela, India. He has pursued his doctoral research in Environmental Biotechnology from Indian Institute of Technology Madras during which he studied biotrickling filtration as a treatment technology to remediate volatile organic pollutants from industrial wastewaters and emissions. He has authored two book chapters and over 20 scientific publications to his credit. His present research areas of interest are in the field of bioenergy, environmental engineering and management, rural technologies and sustainable development. Currently, he is handling two sponsored research projects on biosensor and biosorption.

References

[1] Bhatnagar A, Sillanpaa M. Utilization of agro-industrial and municipal waste materials as potential adsorbents for water treatment – a review. Chem Eng J. 2010;157:277–296.
[2] Solomon LH, Balachandran UN, Mesfin RA, et al. Preparation and characterization of cationic surfactant modified zeolite adsorbent material for adsorption of organic and inorganic industrial pollutants. J Environ Chem Eng. 2017;5:3319–3329.
[3] Rangabhashiyam S, Suganya E, Selvaraju N, et al. Significance of exploiting non-living biomaterials for the biosorption of wastewater pollutants. World J Microbiol Biotechnol. 2014;30:1669–1689.
[4] Kumar SS, Balasubramanian P, Swaminathan G. Degradation potential of free and immobilized cells of white rot fungus *Phanerochaete chrysosporium* on synthetic dyes. Int J Chem Tech Res. 2013;5:565–571.
[5] Haibibu X, Seda C, Deniz B. Removal of some heavy metals onto mechanically activated fly ash: modeling approach for optimization, isotherms, kinetics and thermodynamics. Process Saf Environ Prot. 2017;109:288–300.
[6] Rangabhashiyam S, Anu N, Selvaraju N. Sequestration of dye from textile industry wastewater using agricultural waste products as adsorbents. J Environ Chem Eng. 2013;1:629–641.
[7] Sadaf S, Bhatti HN. Batch and fixed bed column studies for the removal of Indosol Yellow BG dye by peanut husk. J Taiwan Inst Chem Eng. 2014;45:541–553.
[8] Rangabhashiyam S, Selvaraju N. Evaluation of the biosorption potential of a novel *Caryota urens* inflorescence waste biomass for the removal of hexavalent chromium from aqueous solutions. J Taiwan Inst Chem Eng. 2015;47:59–70.
[9] Kim SY, Jin MR, Chung CH, et al. Biosorption of cationic basic dye and cadmium by the novel biosorbent *Bacillus catenulatus* JB-022 strain. J Biosci Bioeng. 2015;119:433–439.
[10] Claudia G, Henrik KH, Piroska H, et al. Biosorption of cadmium with brown macroalgae. Chemosphere. 2015;138:164–169.
[11] Tao S, Jinsong L, Xin B, et al. Biosorption of cadmium ions from aqueous solution by modified *Auricularia Auricular* matrix waste. J Mol Liq. 2017;241:1023–1031.
[12] Milos K, Miljana R, Jelena M, et al. Using xanthated *Lagenaria vulgaris* shell biosorbent for removal of Pb(II) ions from wastewater. J Iran Chem Soc. 2014;11:565–578.

[13] Ehsan D, Masoud K, Mohammad SS, et al. Biosorption of three acid dyes by the brown macroalga *Stoechospermum marginatum*: isotherm, kinetic and thermodynamic studies. Chem Eng J. 2012;195-196:297–306.
[14] He J, Chen JP. A comprehensive review on biosorption of heavy metals by algal biomass: materials, performances, chemistry, and modeling simulation tools. Bioresour Technol. 2014;160:67–78.
[15] Ehsan D, Masoud KMJ, Negin K, et al. Acidic dye biosorption onto marine brown macroalgae: isotherms, kinetic and thermodynamic studies. Chem Eng J. 2012;204-206:225–234.
[16] Lee YC, Chang SP. The biosorption of heavy metals from aqueous solution by *Spirogyra* and *Cladophora* filamentous macroalgae. Bioresour Technol. 2011;102:5297–5304.
[17] Cao D, Xie P, Deng J, et al. Effects of Cu^{2+} and Zn^{2+} on growth and physiological characteristics of green algae, *Cladophora*. Environ Sci Pollut Res. 2015;22:16535–16541.
[18] Dumitru B, Laura B. Equilibrium and kinetics studies of heavy metal ions biosorption on green algae waste biomass. Bioresour Technol. 2012;103:489–493.
[19] Rangabhashiyam S, Anu N, Giri Nandagopal MS, et al. Relevance of isotherm models in biosorption of pollutants by agricultural byproducts. J Environ Chem Eng. 2014;2:398–414.
[20] Langmuir I. The adsorption of gases on plane surfaces of glass, mica and platinum. J Am Chem Soc. 1918;40:1361–1403.
[21] Hall KR, Eagleton LC, Acrivos A, et al. Pore and solid diffusion kinetics in fixed bed adsorption under constant pattern conditions. Ind Eng Chem Fund. 1966;5:212–223.
[22] Freundlich H, Heller W. The adsorption of *cis*- and *trans*-azobenzene. J Am Chem Soc. 1939;61:2228–2230.
[23] Kiselev AV. Vapor adsorption in the formation of adsorbate molecule complexes on the surface. Kolloid Zhur. 1958;20:338–348.
[24] Frumkin AN. Electrocapillary curve of higher aliphatic acids and the state equation of the surface layer. Int J Res Phys Chem Chem Phys. 1925;116:466–488.
[25] Jovanovic DS. Physical adsorption of gases. I: isotherms for monolayer and multilayer adsorption. Colloid Polym Sci. 1969;235:1203–1214.
[26] Lagergren S. About the theory of so-called adsorption of soluble substances. K Svenska Vetenskapsakad Handl. 1898;24:1–39.
[27] Ho YS, McKay G. Pseudo-second order model for sorption processes. Process Biochem. 1999;34:451–465.
[28] Ritchie AG. Alternative to the elovich equation for the kinetics of adsorption of gases on solids. J Chem Soc Faraday Trans. 1977;73:1650–1653.
[29] Weber WJ, Morris JC. Advances in water pollution research: removal of biologically resistant pollutants from waste waters by adsorption. Proceedings of international conference on water pollution symposium. Oxford. Pergamon Press, 1962; vol. 2: p. 231–266.
[30] Rangabhashiyam S, Suganya E, Lity AV, et al. Equilibrium and kinetics studies of hexavalent chromium biosorption on a novel green macroalgae *Enteromorpha* sp. Res Chem Intermed. 2016;42:1275–1294.
[31] Rajesh Kannan R, Rajasimman M, Rajamohan N, et al. Brown marine algae *turbinaria conoides* as biosorbent for malachite green removal: equilibrium and kinetic modeling. Front Environ Sci Eng. 2010;4:116–122.
[32] Rangabhashiyam S, Selvaraju N. Efficacy of unmodified and chemically modified *Swietenia mahagoni* shells for the removal of hexavalent chromium from simulated wastewater. J Mol Liq. 2015;209:487–497.
[33] Bozbas SK, Boz Y. Low-cost biosorbent: *Anadara inaequivalvis* shells for removal of Pb(II) and Cu (II) from aqueous solution. Process Saf Environ Prot. 2016;103:144–152.
[34] Mishra A, Dubey A, Shinghal S. Biosorption of chromium(VI) from aqueous solutions using waste plant biomass. Int J Environ Sci Technol. 2015;12:1415–1426.
[35] Yi Y, Lv J, Liu Y, et al. Synthesis and application of modified Litchi peel for removal of hexavalent chromium from aqueous solutions. J Mol Liq. 2017;225:28–33.

[36] Fatemeh M, Elnaz K, Leila A, et al. Nickel and lead biosorption by *Curtobacterium* sp. FM01, an indigenous bacterium isolated from farmland soils of northeast Iran. J Environ Chem Eng. 2016;4:950–957.
[37] Onyancha D, Mavura W, Ngila JC, et al. Studies of chromium removal from tannery wastewaters by algae biosorbents, *Spirogyra condensata* and *Rhizoclonium hieroglyphicum*. J Hazard Mater. 2008;158:605–614.
[38] Gupta VK, Rastogi A. Biosorption of hexavalent chromium by raw and acid-treated green alga *Oedogonium hatei* from aqueous solutions. J Hazard Mater. 2009;163:396–402.
[39] Rangabhashiyam S, Selvaraju N. Adsorptive remediation of hexavalent chromium from synthetic wastewater by a natural and $ZnCl_2$ activated *Sterculia guttata* shell. J Mol Liq. 2015;207:39–49.
[40] Kuppusamy S, Thavamani P, Megharaj M, et al. Potential of *Melaleuca diosmifolia* leaf as a low-cost adsorbent for hexavalent chromium removal from contaminated water bodies. Process Saf Environ Prot. 2016;100:173–182.
[41] Khosravi R, Fazlzadehdavil M, Barikbin B, et al. Removal of hexavalent chromium from aqueous solution by granular and powdered *Peganum Harmala*. Appl Surf Sci. 2014;292:670–677.
[42] Vasanth Kumar K, Sivanesan S, Ramamurthi V. Adsorption of malachite green onto Pithophora sp., a fresh water algae: equilibrium and kinetic modelling. Process Biochem. 2005;40:2865–2872.
[43] Dahri MK, Rahimi Kooh MR, Lim LBL. Water remediation using low cost adsorbent walnut shell for removal of malachite green: equilibrium, kinetics, thermodynamic and regeneration studies. J Environ Chem Eng. 2014;2:1434–1444.
[44] Guechi EK, Hamdaoui O. Sorption of malachite green from aqueous solution by potato peel: kinetics and equilibrium modeling using non-linear analysis method. Arab J Chem. 2016;9:S416–S424.
[45] Gunduz F, Bayrak B. Biosorption of malachite green from an aqueous solution using pomegranate peel: equilibrium modelling, kinetic and thermodynamic studies. J Mol Liq. 2017;243:790–798.
[46] Rangabhashiyam S, Lata S, Balasubramanian P. Biosorption characteristics of methylene blue and malachite green from simulated wastewater onto *Carica papaya* wood biosorbent. Surf Interfaces. 2017. DOI:10.1016/j.surfin.2017.09.011.
[47] Vijayaraghavan K, Rangabhashiyam S, Ashokkumar T, et al. Assessment of samarium biosorption from aqueous solution by brown macroalga *Turbinaria conoides*. J Taiwan Inst Chem Eng. 2017;74:113–120.
[48] Daneshvar E, Vazirzadeh A, Niazi A, et al. A comparative study of methylene blue biosorption using different modified brown, red and green macroalgae – effect of pretreatment. Chem Eng J. 2017;307:435–446.
[49] Flores-Chaparro CE, Chazaro Ruiz LF, Alfaro de la Torre MC, et al. Biosorption removal of benzene and toluene by three dried macroalgae at different ionic strength and temperatures: algae biochemical composition and kinetics. J Environ Manage. 2017;193:126–135.